

Enhanced Variational Quantum Kolmogorov-Arnold Network

Hikaru Wakaura ^{1,*}, Rahmat Mulyawan ^{2,3,/}, and Andriyan B. Suksmono ^{2,3,4,+}

¹QuantScape Inc. QuantScape Inc., 4-11-18, Manshon-Shimizudai, Meguro, Tokyo, 153-0064, Japan

²The School of Electrical Engineering and Informatics, Institut Teknologi Bandung (STEI-ITB), Jl. Ganesha No.10, Bandung, Indonesia

³Research Collaboration Center for Quantum Technology 2.0, BRIN-ITB-TelU, Indonesia

⁴ITB Research Center on ICT (PPTIK-ITB)

*hikaruwakaura@gmail.com

/rahmat.mulyawan@itb.ac.id

+suksmono@itb.ac.id

ABSTRACT

The Kolmogorov-Arnold Network (KAN) is a novel multi-layer network model recognized for its efficiency in neuromorphic computing, where synapses between neurons are trained linearly. Computations in KAN are performed by generating a polynomial vector from the state vector and layer-wise trained synapses, enabling efficient processing. While KAN can be implemented on quantum computers using block encoding and Quantum Signal Processing, these methods require fault-tolerant quantum devices, making them impractical for current Noisy Intermediate-Scale Quantum (NISQ) hardware. We propose the Enhanced Variational Quantum Kolmogorov-Arnold Network (EVQKAN) to overcome this limitation, which emulates KAN through variational quantum algorithms. The EVQKAN ansatz employs a tiling technique to emulate layer matrices, leading to significantly higher accuracy compared to conventional Variational Quantum Kolmogorov-Arnold Network (VQKAN) and Quantum Neural Networks (QNN), even with a smaller number of layers. EVQKAN achieves superior performance with a single-layer architecture, whereas QNN and VQKAN typically struggle. Additionally, EVQKAN eliminates the need for Quantum Signal Processing, enhancing its robustness to noise and making it well-suited for practical deployment on NISQ-era quantum devices.

1 Introduction

The rapid advancements in artificial intelligence (AI) have been largely driven by neural network models inspired by the structure of the human brain¹. These models, consisting of interconnected artificial neurons or perceptrons^{2,3}, have demonstrated remarkable success in various applications, including image recognition and natural language processing⁴. However, traditional neural networks face significant scalability and computational efficiency limitations when processing large-scale data, which hampers further advancements in AI. To overcome these challenges, researchers have explored alternative network architectures. One particularly promising approach is the Kolmogorov-Arnold Network (KAN), recently proposed by Tegmark's group⁵. KAN improves computational efficiency by optimizing synaptic weights by directly manipulating neuron parameters, utilizing matrix operations for more efficient computation. Furthermore, its design allows for interpretation and implementation as a quantum circuit, facilitating seamless integration between quantum computing and neural network models. Consequently, research on the theory and applications of KAN has gained significant momentum globally, with many groups actively investigating its potential across various domains. Though there are some critical opinions⁶, there is already a lot of research reported, for example, image analysis⁷, time-dependent analysis⁸, and solving problems in physics^{9,10}. KAN is good at solving. Furthermore, it is applied for controlling spacecraft and medical use^{11,12}.

In this context, KAN for use on quantum computers has been studied since the show of KAN. Quantum computers are novel computers that utilize quantum superposition states proposed by Richard P. Feynman. They can solve some kinds of problems, such as classical computers taking exponential time for the amount of data in polynomial time by well-known quantum algorithms. Their power is from superposition state and memory space 2^{N_q} sized for the number of qubits N_q , which is the unit of quantum discrete information. Hence, KAN promises to be able to calculate a large multi-layer network using the power of quantum computers.

The KAN complies with the manner of Variational Quantum Algorithms (VQAs) called Variational Quantum KAN¹³, and Quantum KAN¹⁴ reproduced on the quantum circuit by the manner of Quantum Signal Processing¹⁵ using block encoding?

technique, which is the quantum algorithms to make given matrices including non-hermitian and rectangle matrices are major.

The KAN optimizes the architecture of a parametric quantum circuit called for Quantum Architecture Search¹⁶ is also released. However, VQKAN's accuracy is not enough for practical use, and Quantum KAN requires many control gates and ancilla qubits; hence, it can not be used correctly on current devices. Furthermore, Quantum KAN requires at least the number of elements of layer matrix parameter functions per layer; hence, the optimization takes a long time, and the number of trials in the process becomes numerous.

Therefore, we propose a novel quantum version of KAN called Enhanced VQKAN (EVQKAN), which abides by the manner of VQAs. VQKAN¹³ is KAN on a variational quantum framework for quantum machine learning that uses measurement results of qubits as neurons and quantum gates as synapses. The framework of VQKAN is the same as that of VQAs. The VQKAN utilizes the multi-layer architecture, parametric gates, and feedback to reproduce the KAN scheme by modifying the Variational Quantum Eigensolver (VQE) scheme. EVQKAN uses the matrices emulating the layer of KAN, and the number of parameter functions is only 2^{N_q-1} for the dimension of layer 2^{N_q} at a maximum. Hence, EVQKAN's accuracy is promised to be higher than that of VQKAN, even though the calculation time becomes longer. Quantum computing algorithms, particularly VQAs, have recently experienced remarkable advancements. Foundational contributions from Aspuru-Guzik and collaborators¹⁷ have paved the way for algorithms such as the Variational Quantum Eigensolver (VQE)¹⁸, Adaptive VQE¹⁹, and Multiscale Contracted VQE (MCVQE)²⁰. These algorithms are highly compatible with Noisy Intermediate-Scale Quantum (NISQ) devices and have found applications in quantum machine learning tasks²¹⁻²⁹. We performed the EVQKAN on the fitting of elementary function and classification of the points on 2-D plane. As a result, EVQKAN demonstrated significant accuracy for both fitting and classification problems compared to Quantum Neural Network (QNN)³⁰ and VQKAN even if the number of layers is only 1. The EVQKAN has the potential to be a practical quantum machine learning algorithm.

Section 1 is the introduction, section 2 describes the method detail of EVQKAN and the optimization method, section 3 describes the result of the fitting and classification problem, Section 4 is the discussion of results, and section 5 is the concluding remark.

2 Method

In this section, we describe the method and implementation of the Enhanced Variational Quantum Kolmogorov-Arnold Network (EVQKAN). VQKAN is the variational quantum algorithm version of KAN, a multi-layer network based on the connection of synapses in neurons. First, initial state $|\Psi_{ini}(\mathbf{x}^m)\rangle$ is $\prod_{j=0}^{N_q-1} Ry^j(\text{acos}(2\mathbf{x}_j^m - 1)) |0\rangle^{\otimes N_q}$ for each input m . $Ry^j(\theta)$ is θ degrees angle rotation gate for y-axis on qubit j . ${}_n\mathbf{x}^m$ is the input vector at layer n for m -th input data. We will describe later that the Loss function is calculated similarly to Subspace-search VQE³¹, and multiple points are calculated at once. For VQKAN, $\phi_{jk}^n({}_n\mathbf{x}^m)$ is the gate of the angle.

$$\phi_{jk}^n({}_n\mathbf{x}^m) = \sum_{i \in \{0, \text{dim}({}_n\mathbf{x}^m)\}}^0 2\text{acos}(E_f({}_n\mathbf{x}_i^m) + \sum_{s=0}^{N_g-1} \sum_{l=0}^{N_s-1} c_s^{njk} B_l({}_n\mathbf{x}_i^m)) \quad (1)$$

, which N_d^n is the number of input for layer n , N_g is the number of grids foreach gate, N_s is the number of splines, respectively. Then, c_s^{njk} and $B_l({}_n\mathbf{x}_i^m)$ are the parameters to be trained, initialized into 0 and spline functions at layer n , respectively, the same as classical KAN. ${}_n\mathbf{x}^m$ is the input vector at layer n , j and k are the index of qubits, respectively. Only one element on ${}_n\mathbf{x}^m$ is chosen for each $\phi_{jk}^n({}_n\mathbf{x}^m)$ on EVQKAN.

$E_f({}_n\mathbf{x}_i^m) = {}_n\mathbf{x}_i^m / (\exp(-{}_n\mathbf{x}_i^m) + 1)$ is the Fermi-Dirac expectation energy-like value of the distribution. The component of ${}_n\mathbf{x}$ is the expectation value of the given observable for the calculated states of qubits. The layer corresponds to the quantum circuit to make a superposition state called ansatz. EVQKAN uses the tiled matrices by the elements of gate operation matrices made by the sum operator and block encoding technics. We use the method of sum operator for tiling, like,

$$U_n^{k, \{0, 2^k-1\}} = U_n^{k-1, \{0, 2^{k-1}-1\}} + U_n^{k-1, \{2^{k-1}, 2^k-1\}} \quad (2)$$

$$X_k U_n^{0,p} = \prod_{j=0}^{N_q} C_j^{N_q-1} Ry^0(\phi_{jp}^n({}_n\mathbf{x}_j^m)) \quad (3)$$

Then, $C_j^k Ry^0$ is the k -qubit controlled y-axis rotation gate with 0 th qubit as target qubit that acts y-axis rotation gate when the control qubits are $|j\rangle$ state for the decimal expression of binary state of qubits and N_q is the number of qubits, respectively.

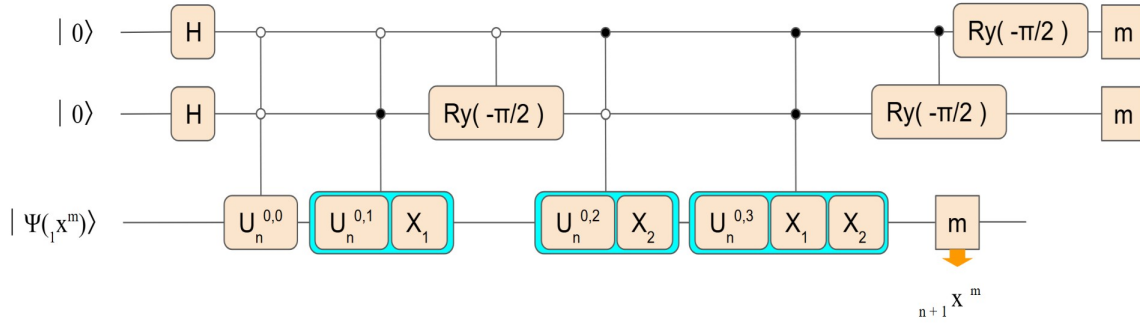


Figure 1. Simplified picture of our ansatz on EVQKAN. White circle indicates that connected operators are acted on the circuit in case the qubits that the circle exists is $|0\rangle$ state and black circle indicates that connected operators are acted on the circuit in case the qubits that the circle exists is $|1\rangle$ state, respectively.

The entire ansatz is,

$$\Phi_n^E = MU_n^{N_q-1, \{0, 2^{N_q-1}-1\}} \quad (4)$$

$$|\Psi(1\mathbf{x}^m)\rangle = \prod_{n=1}^{\text{num. of layers } N_l} \Phi_n^E M |\Psi_{ini}(1\mathbf{x}^m)\rangle \quad (5)$$

We implement the technique for implementation of sum operators by the manners on paper³². The illustrated circuit of a single layer is as Fig.1. We will demonstrate solving fitting problems of elementary equations and classification using the example of $N_q = 3$. Sum operators are gained in case the measurement result of ancillary qubits are all zero state. For working qubits, the state of the qubits is destroyed after measurement, and calculations commence from scratch using the measured input vector, omitting m gates in case calculations are done on real devices. We save the states for easiness because the demonstrations on the paper are all numerical simulations.

Others are the same as ordinary VQKAN¹³.

The result is readout as a form of the Hamiltonian expectation value H , and the loss function is calculated as follows,

$$l_m = |\langle \Psi(1\mathbf{x}^m) | H | \Psi(1\mathbf{x}^m) \rangle - f^{aim}(1\mathbf{x}^m)| \quad (6)$$

$$L = \sum_{m=0}^{\text{num. of samples } N-1} a_m l_m \quad (7)$$

where $f^{aim}(1\mathbf{x}^m)$ is the aimed value of sampled point m and l_m is the loss function (absolute distance) of point m , respectively. Hamiltonian takes the form $H = \sum_{j=0}^{N_o-1} \theta_j P_j$ for the product of the Pauli matrix P_j , consisting of the Pauli matrix X_j, Y_j, Z_j . N_o is the number of P_j in Hamiltonian.

The condition of convergence is the default of scipy for all methods. We assume $N = 10, a_m = (N - m)/N, N_l = 3, N_q = 3, N_g = 8$ and $N_s = 4(tr + 2)$ for the number of trials tr , respectively. We use blueqat SDK³³ for numerical simulation of quantum calculations and COBYLA of scipy to optimize parameters but to declare the use of others. We assume that the number of shots is infinite. All calculations except declaration are performed in Jupyter notebook with Anaconda 3.9.12 and Intel Core i7-9750H.

3 Result

In this section, we show the EVQKAN result on fitting the elemental equation and classifying points on the 2D plane. The number of ϕ s is 16 per layer, and the number of qubits, including ancillae, is 8, respectively. We performed the EVQKAN of the following equation on 10 sampled points and predicted the values of 50 test points after optimization by sampled points.

3.1 Fitting problem

First, we describe the result of the fitting problem. The target function is defined as:

$$f^{\text{aim}}(\mathbf{x}) = \exp(\sin(x_0^2 + x_1^2) + \sin(x_2^2 + x_3^2)). \quad (8)$$

Here, ${}_n\mathbf{x}_{2i}^m = 0.5(\langle \tilde{\Psi}(\mathbf{x}^m) | Z_{2i} | \tilde{\Psi}(\mathbf{x}^m) \rangle + 1)$ and ${}_n\mathbf{x}_{2i+1}^m = 0.5(\langle \tilde{\Psi}(\mathbf{x}^m) | Y_{2i+1} | \tilde{\Psi}(\mathbf{x}^m) \rangle + 1)$ which the realm is normalized in $\{0, 1\}$ for the state calculated by n-th layer $|\tilde{\Psi}(\mathbf{x}^m)\rangle$, with $N_d^n = 4$ and $\dim({}_n\mathbf{x}^m) = 4$ for all layers and calculations, and the Hamiltonian is $Z_0 Z_1$. Initial state on solving fitting problem is $|\Psi_{\text{ini}}(\mathbf{x}^m)\rangle$ is $\prod_{j=0}^{N_q-1} R_y^j(\text{acos}(2{}_1\mathbf{x}_{2j}^m - 1)) R_x^j(\text{acos}(2{}_1\mathbf{x}_{2j+1}^m - 1)) |0\rangle^{\otimes N_q}$.

In advance, we show the result for QNN, VQKAN, Adaptive VQKAN³⁴, respectively.

The QNN ansatz consists of three layers, as shown in Fig. 2, with a total of 24 parameters initialized randomly. The initial state is $|0\rangle^{\otimes N_q}$.

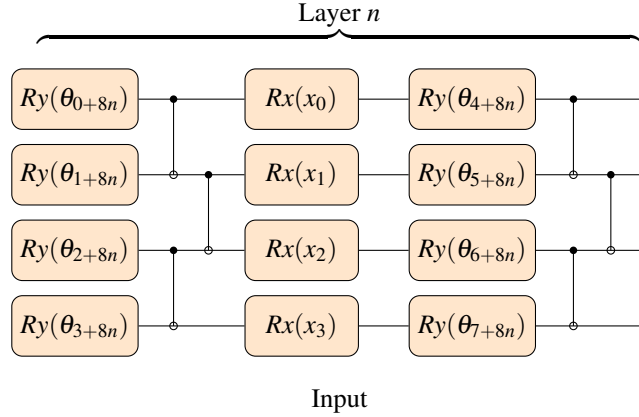


Figure 2. Ansatz structure of the Quantum Neural Network (QNN) with parameterized rotation gates controlled by trainable parameters θ_j . Inputs x_i encode classical data into the quantum circuit, enabling learning through optimization of θ_j to minimize the cost function.

Fig. 3 (a) shows the convergence of the loss function over the number of trials for 10 attempts, while Fig. 4 (blue line) presents the fitting results on the test points of QNN.

The loss functions of half of ten attempts reached below 0.5. However, the average sum of the difference between the absolute value of aimed and calculated value of points (absolute distances) is over 25 as also shown in Table.1. According to the values of the loss function, QNN is not good at fitting the equation using the same encoding as EVQKAN and is trapped by overfitting because the average of the absolute distances on each point is nearly 1 even though their minimums are small.

Fig. 3 (b) and (c) shows the convergence of the loss function over the number of trials for 10 attempts, while Fig. 4 (green line) and (orange line) presents the fitting results on the test points of VQKAN and Adaptive VQKAN, respectively.

The ansatz of VQKAN is 3 layer canonical ansatz and the initial absatz of Adaptive VQKAN is X_0 , respectively. The initial parameters are all zero and $N_g = 8$ the same as EVQKAN , and the number of epochs of Adaptive VQKAN is 15 which the number of trials of optimizer for each epoch is 1000, respectively. Absolute distances are entirely smaller than those of QNN and a little larger than those of EVQKAN even though the loss functions are larger than that of QNN.

Next, we show the result of fitting by EVQKAN on Figs. 3 (d) and 3 (red line).

Fig. 3 (d) shows the convergence of the loss function over the number of trials for 10 attempts, while Fig. 4 (red line) presents the fitting results on the test points. The values loss functions on seven of ten attempts are below 0.5 even though they had not converged yet. The average of the sum of the absolute distances is nearly 15 which is about 10 smaller than that of QNN. The result of fitting on test points shows a little overfitting because the absolute distances on some test points are below

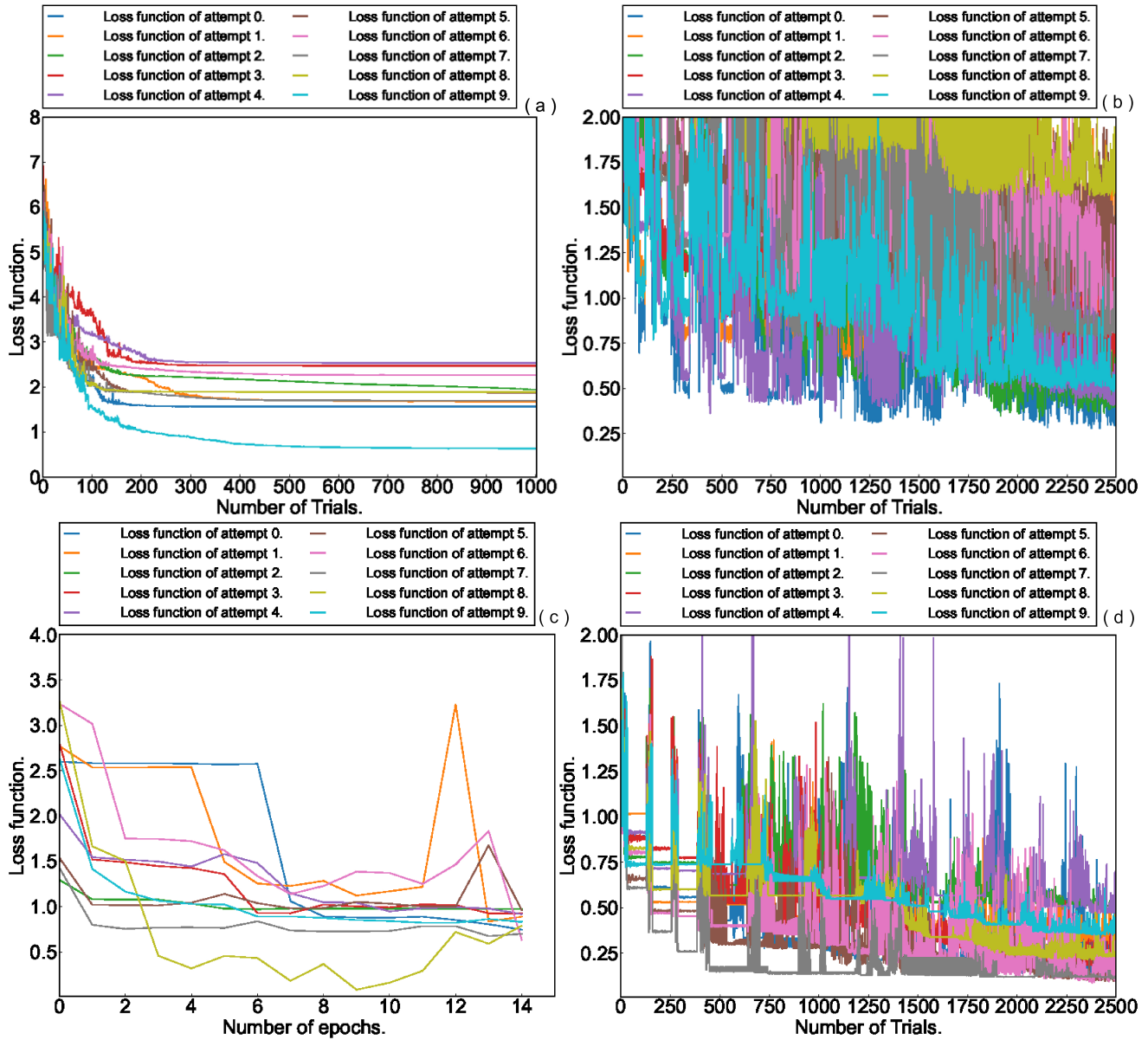


Figure 3. Number of trials vs. loss functions for optimization of the fitting problem by (a) QNN, (b) VQKAN, (c) Adaptive VQKAN, and (d) Enhanced VQKAN, respectively.

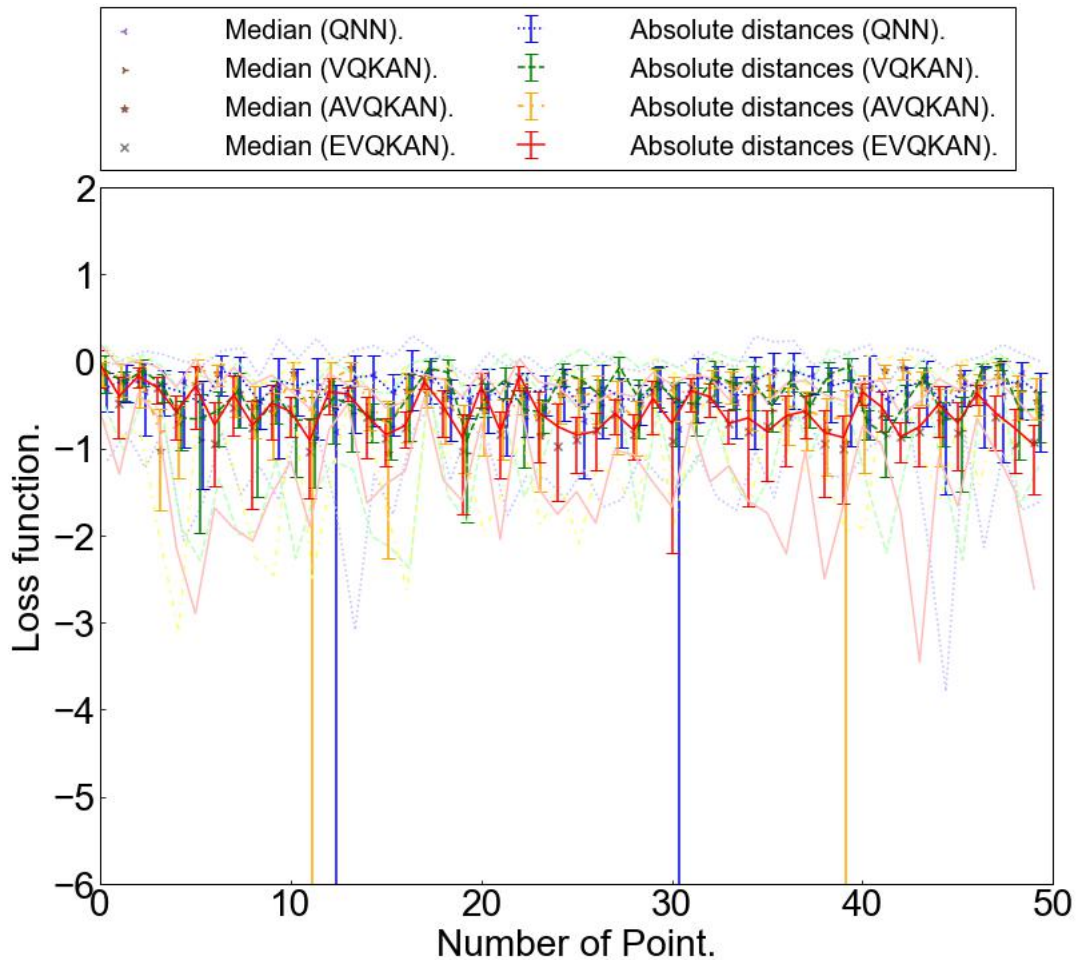


Figure 4. (Right) Number of test points vs. average and median of loss functions (absolute distances) in log10 scale of test points on (blue line) QNN, (green line) VQKAN, (orange line) Adaptive VQKAN, and (red line) Enhanced VQKAN optimization, respectively. The line of QNN, VQKAN, and Adaptive VQKAN, are moved right 0.375, 0.25, and 0.125, respectively.

Table 1. Averages, medians, minimums, and maximums of the sum of absolute distances for QNN, VQKAN, Adaptive VQKAN, and EVQKAN, which $N_l = 3$ for all methods for 10 attempts using COBYLA.

Method	Sum Abs. Dist. Ave.	Sum Abs. Dist. Med.	Sum Abs. Dist. Min.	Sum Abs. Dist. Max.
QNN	25.965271	25.688473	14.535198	35.561974
VQKAN	22.609012	22.95691	19.876415	24.682033
AVQKAN	22.380898	21.933966	16.90373	28.293902
EVQKAN	15.088392	15.118825	13.120516	18.640238

0.01, and some are above 0.1, even though the averages on test points are entirely smaller than those of QNN. The EVQKAN is supposed to be good at predicting learned points in optimization.

Table.1 shows the detail of the sum of absolute distances for QNN, VQKAN, and EVQKAN. The average of the sum of absolute distances on EVQKAN is far smaller than that of QNN and VQKAN because the maximum on QNN is over 16 larger than that of EVQKAN, and the minimum on VQKAN is over 6 larger than that of EVQKAN, respectively. Besides, the sum of absolute distances on QNN on three of ten attempts are over 30.

3.2 Classification problem

In this section, we present the results of solving the classification problem for points on a 2-D plane. A point is assigned a label of +1 if it is above the function f and -1 if it is below f . The function f is defined as:

$$f(x) = \exp(d_0x_0 + d_1) + d_2\sqrt{1 - d_3x_0^2} + \cos(d_4x_0 + d_5) + \sin(d_6x_0 + d_7) \quad (9)$$

where d_k represents random coefficients between 0 and 1 for the various cases. The loss function for the classification is given as follows:

$$f^{\text{aim}} = \begin{cases} -1 & \text{if } f \geq x_1 \\ 1 & \text{if } f < x_1 \end{cases} \quad (10)$$

We show the results of the classification for different cases: using QNN with $\dim(n, \mathbf{x}^m) = 2$, and using EVQKAN with $\dim(n, \mathbf{x}^m) = 2$ for $n > 2$ for 10 attempts.

In advance, we show the result for QNN.

Fig. 6 (a) shows the loss functions for different attempts, while Fig. 7 (blue line) displays the classification results for 50 randomly sampled points.

The calculation has not converged to a global value, and the sum of absolute distances is also large, at an average of 30.160192, as also shown in Table.2. 40 test points are classified correctly concerning the sign of average of absolute distance.

Fig. 6 (b) and (c) shows the convergence of the loss function over the number of trials for 10 attempts, while Fig. 7 (green line) and (orange line) presents the fitting results on the test points of VQKAN and Adaptive VQKAN, respectively.

The absolute distances of both are larger than that of QNN. Furthermore, absolute distances of Adaptive VQKAN are the largest because the ansatz is never grown. The values of loss functions are larger than those of QNN.

Next, we show the result of classification by EVQKAN on Figs. 6 (d) and 7 (red line).

Fig. 6 (d) shows the convergence of the loss function over the number of trials for 10 attempts, while Fig. 7 (red line) presents the results of classification on the test points.

The loss functions on attempts were not converged. Besides, the average of the sum of absolute distances is a little below that of QNN. Correctly classified test points are 38 points, fewer than QNN's. EVQKAN also shows the overfitting for classification problems. EVQKAN is supposed to require more number of parameters to calculate more accurately, and the accuracy on learned points is more significant than QNN. According to Table.2, EVQKAN has a smaller average and larger median than QNN because the major number of points on QNN are 20 at a minimum and 30 at a maximum sum, which is 10 smaller than EVQKAN's. VQKAN has the largest average; hence, the prediction accuracy is improved by applying the ansatz of EVQKAN.

EVQKAN may calculate more accurately in case $N = 20$ as ordinary VQKAN.

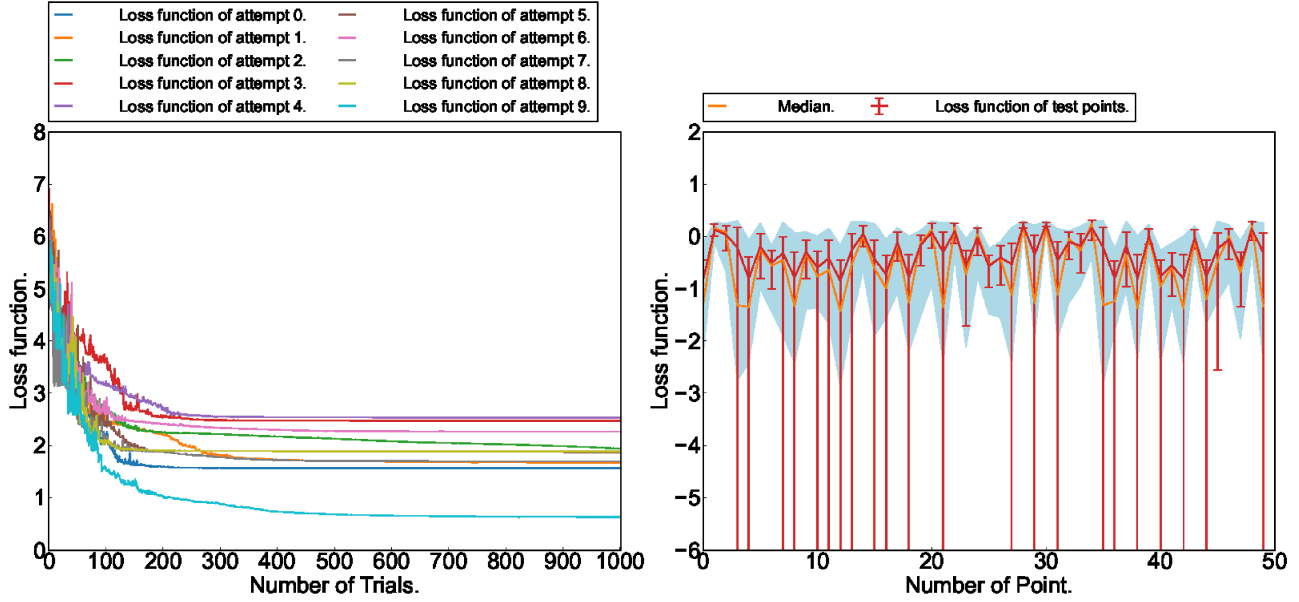


Figure 5. (Left) Number of trials vs. loss functions for attempts on classification problem using QNN. (Right) Number of test points vs. the average and median loss functions (absolute distances) of test points using QNN optimization.

Table 2. Averages, medians, minimums, and maximums of the sum of absolute distances for QNN, VQKAN, Adaptive VQKAN, and EVQKAN, which $N_l = 3$ for all methods for 10 attempts using COBYLA.

Method	Sum Abs. Dist. Ave.	Sum Abs. Dist. Med.	Sum Abs. Dist. Min.	Sum Abs. Dist. Max.
QNN	30.160192	26.056678	18.386881	47.954906
VQKAN	41.981422	42.469602	35.759268	49.323569
AVQKAN	49.731165	49.638376	48.781257	51.608939
EVQKAN	29.627604	32.453662	17.349453	39.013591

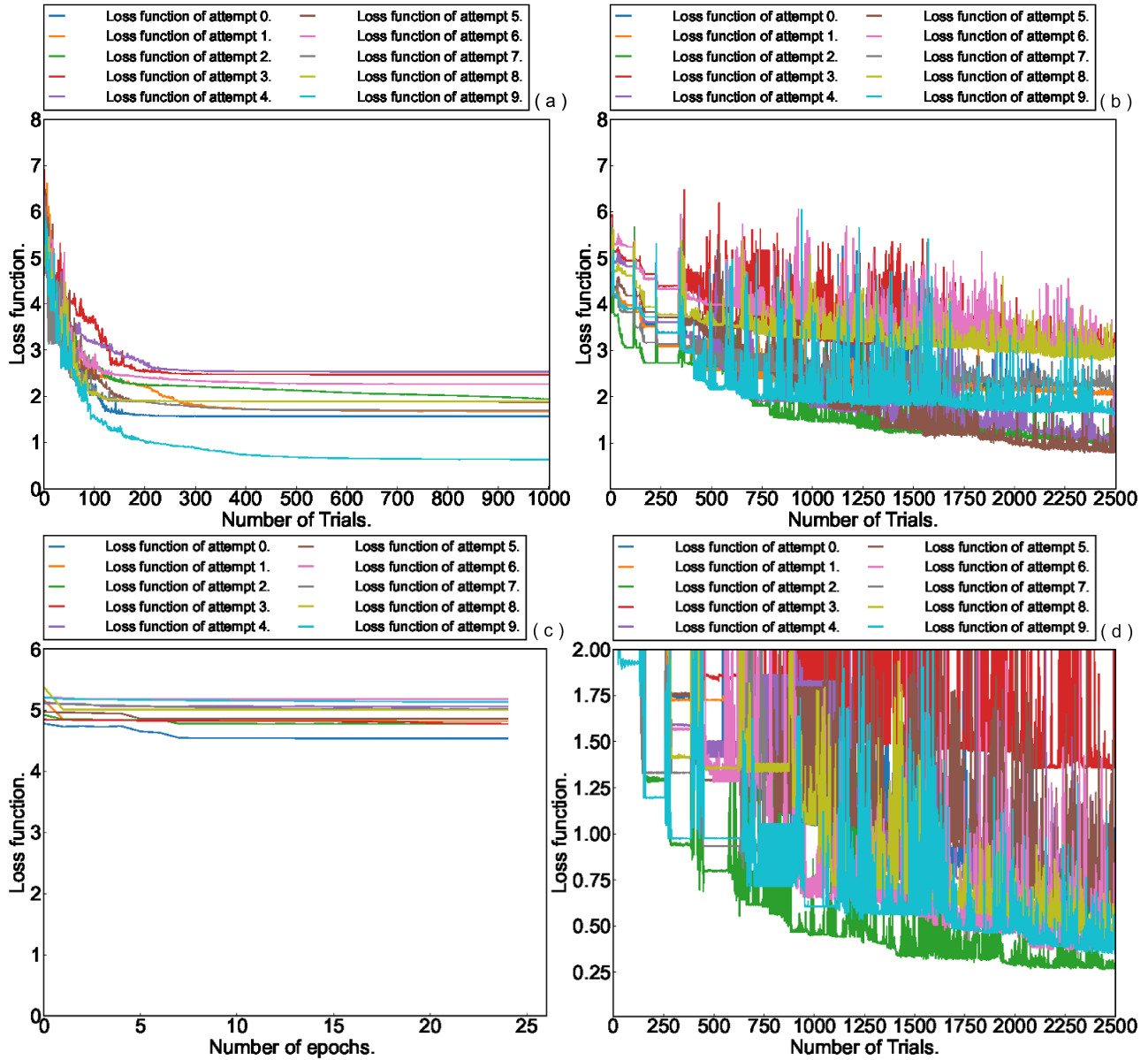


Figure 6. Number of trials vs. loss functions for optimization of the classification problem by (a) QNN, (b) VQKAN, (c) Adaptive VQKAN, and (d) Enhanced VQKAN, respectively.

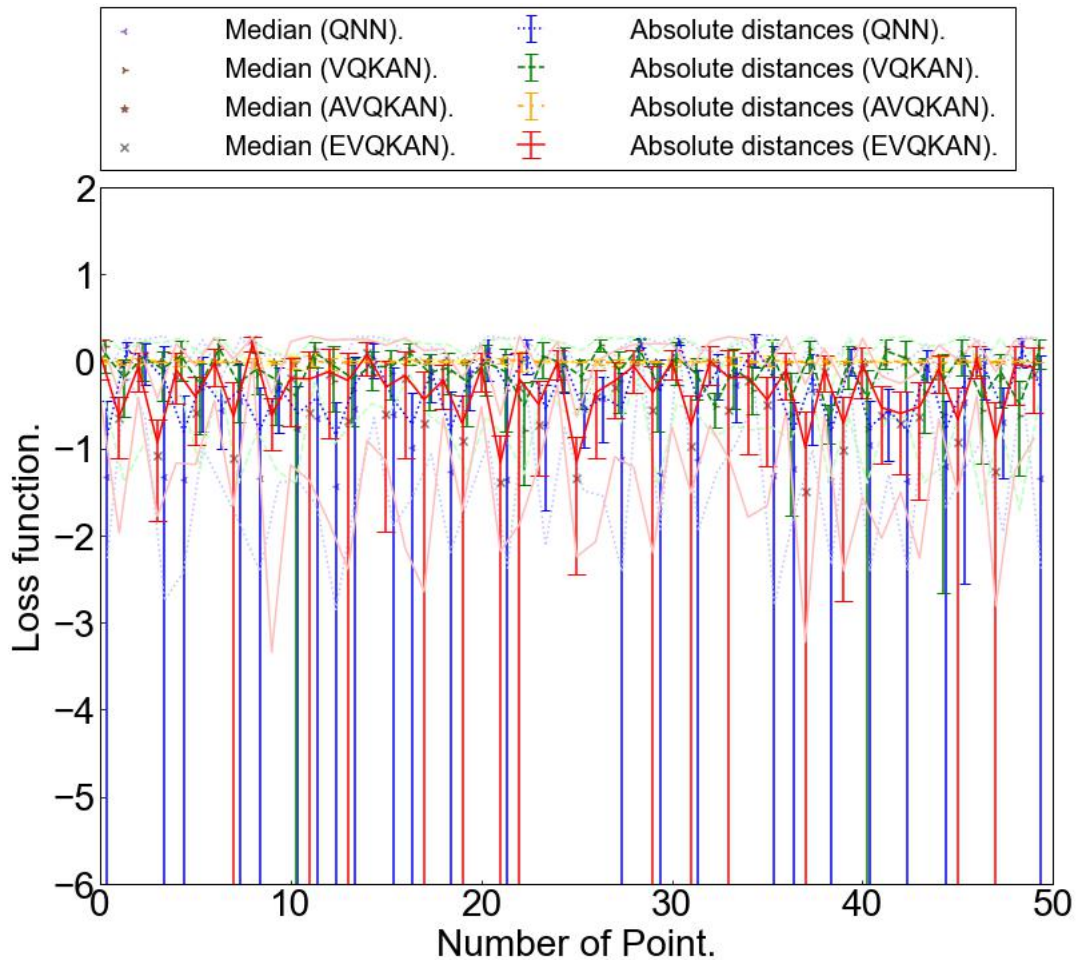


Figure 7. (Right) Number of test points vs. average and median of loss functions (absolute distances) in log10 scale of test points on (blue line) QNN, (green line) VQKAN, (orange line) Adaptive VQKAN, and (red line) Enhanced VQKAN optimization, respectively. The line of QNN, VQKAN, and Adaptive VQKAN, are moved right 0.375, 0.25, and 0.125, respectively.

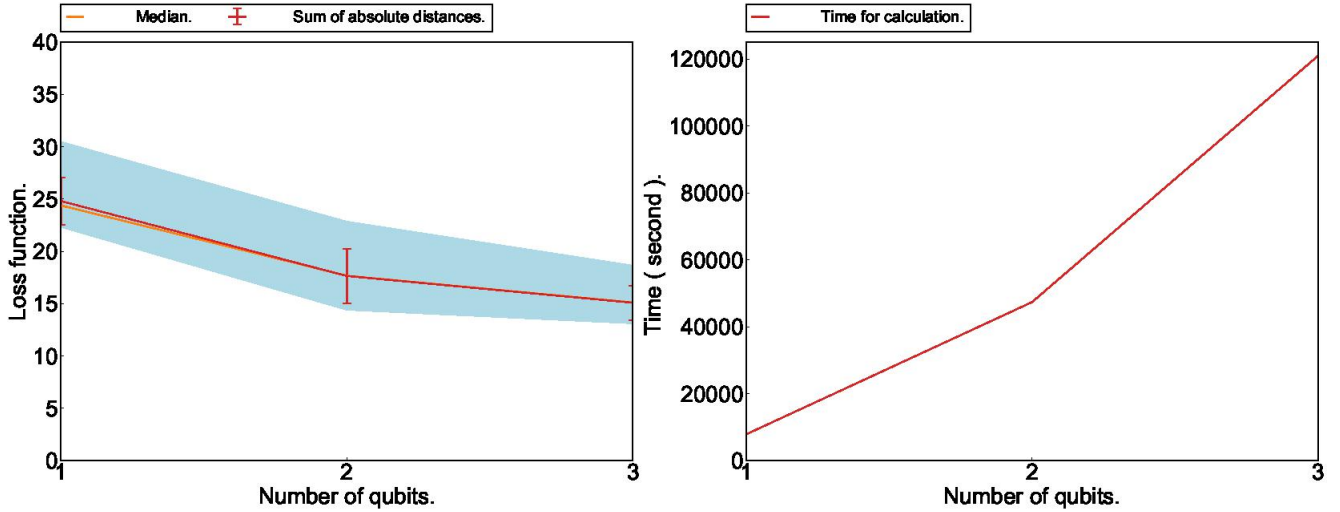


Figure 8. (Left) Number of layers vs. sum of absolute distances using EVQKAN on fitting problem with $N_q = 3$ and COBYLA.(Right) Number of layers vs. elapsed time.

4 Discussion

In this section, we discuss the key findings in this work, focusing on the accuracy and time required to calculate EVQKAN for the fitting and classification problem. Firstly, we discuss the accuracy and time of fitting problems, including the reason and the way to improve them. Fig.8 (Left) shows the average of the sum of absolute distances of 50 test points; those are the result of prediction after optimization of EVQKAN on the fitting problem for the number of layers, while (Right) shows the calculation time. The average is a little smaller than that of QNN when the number of layers is 1 and declines drastically as the number of layers increases. The average may be nearly zero when the number of layers is above 6. However, the calculation time increases nearly exponentially saturating. This is because the circuit for calculating the sum operator requires 20 n-bit Toffoli gates, and 16 of them require 4-bit Toffoli gates. Besides, our implementation of 4-bit Toffoli gate uses 3 extra ancilla qubits. The other way to implement our circuit of EVQKAN may accelerate the calculation, for example, block encoding and qubitization can realize it. Block encoding simplified the circuit for calculating the matrix function on quantum computers. Tensor product³⁵ decomposition may also accelerate calculation and save the number of qubits. Our ansatz includes one input vector element per row. Hence, the state vectors of EVQKAN include only one input vector element per element. The transposed ansatz includes all their elements; hence, the accuracy of EVQKAN can improve. Fig. 9 (Left) shows the convergence of the loss function over the number of trials for 10 attempts in case the ansatz is transposed and the number of layers is only 1, while Fig. 9 (Right) presents the fitting results on the test points.

Though the loss functions are larger than that of ordinary ansatz, the absolute distances of test points have smaller values entirely than those of ordinary ansatz, even if the number of layers is only 1.

Furthermore, the average of the sum of the absolute distances is smaller than that in case the ansatz is ordinary and the number of layers is 1, and QNN in case the number of layers is 3 as shown in Tables.1 and 3. In addition, they are as small as those of VQKAN and Adaptive VQKAN.

Table 3. Averages, medians, minimums, and maximums of the sum of absolute distances for conventional and transposed ansatz in case the number of layers is 1, along with computation times (seconds) for 10 attempts using COBYLA.

Ansatz	Sum Abs. Dist. Ave.	Sum Abs. Dist. Med.	Sum Abs. Dist. Min.	Sum Abs. Dist. Max.	Time (second)
conventional	24.819239	24.394783	22.347493	30.467566	7810
transposed	22.93362	22.959923	20.798762	24.696152	7571

Next, we discuss the accuracy and time of the classification problem. Fig.10 (Left) shows the average of the sum of absolute distances of 50 test points; those are the result of prediction after optimization of EVQKAN on classification problem for the number of layers, while (Right) shows the calculation time. The average is larger than that of QNN when the number of layers is 1 and declines as the number of layers increases. However, a decline of the average saturates at 3.

Other modifications are required to improve the accuracy, such as changing the $dim(n\mathbf{x}^m)$ after the second layer and the number of sampled points. Besides, the calculation time increases nearly exponentially, saturating the same as fitting. Block

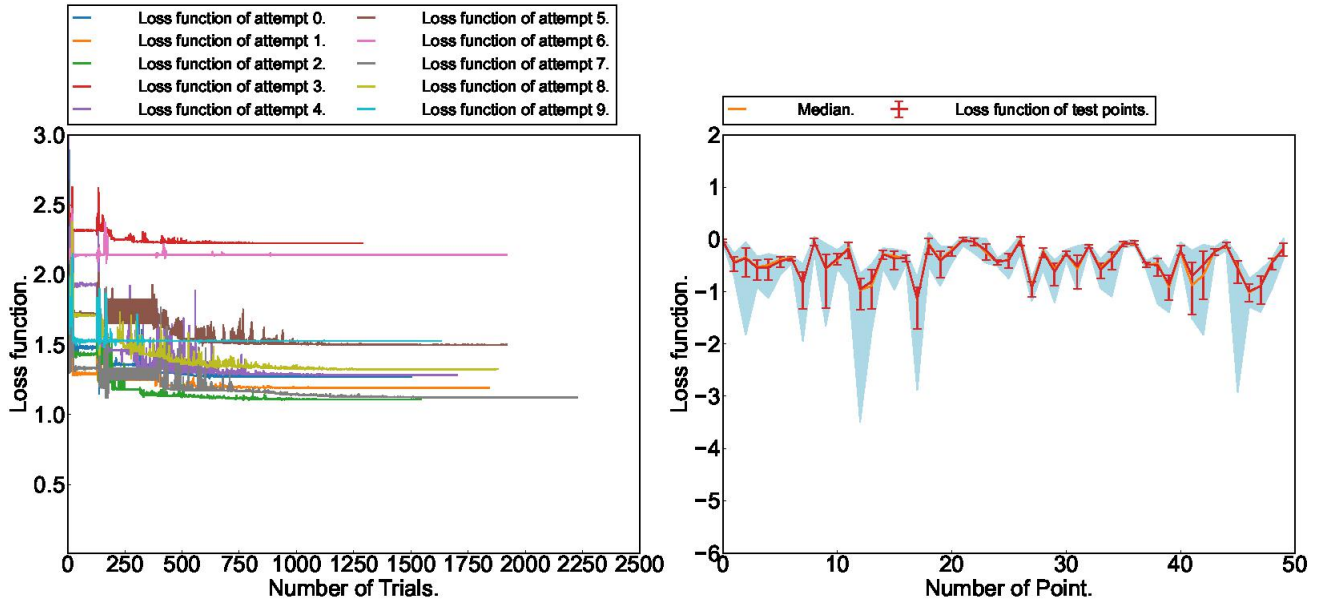


Figure 9. (Left) Number of trials vs. loss functions for optimization attempts on the fitting problem by EVQKAN in case the ansatz is transposed and the number of layers is 1. (Right) Number of test points vs. average and median of loss functions (absolute distances) in log10 scale of test points on EVQKAN optimization.

encoding and qubitization may contribute to calculation time.

Fig. 11 (Left) shows the convergence of the loss function over the number of trials for 10 attempts in case the ansatz is transposed and the number of layers is only 1, while Fig. 11 (Right) presents the classification results on the test points. Though the loss functions are larger than that of ordinary ansatz, the absolute distances of test points have smaller values entirely than those of ordinary ansatz, even if the number of layers is only 1. Furthermore, the average of the sum of the absolute distances is smaller than that in case the ansatz is ordinary, QNN and EVQKAN in case the number of layers is 3 as shown in Tables.2 and 4. The QNN has low accuracy in case the number of layers is 1^{36,37}, thus, exhibits the prominent accuracy and potential for practical use. Besides, EVQKAN requires fewer trials for convergence than QNN; thus, it can be faster and more robust to noise.

Table 4. Averages, medians, minimums, and maximums of the sum of absolute distances for conventional and transposed ansatz in case the number of layers is 1, along with computation times (seconds) for 10 attempts using COBYLA.

Ansatz	Sum Abs. Dist. Ave.	Sum Abs. Dist. Med.	Sum Abs. Dist. Min.	Sum Abs. Dist. Max.	Time (second)
conventional	48.105533	45.816094	37.844375	60.291046	6296
transposed	26.993835	24.444128	19.672796	44.55341	8541

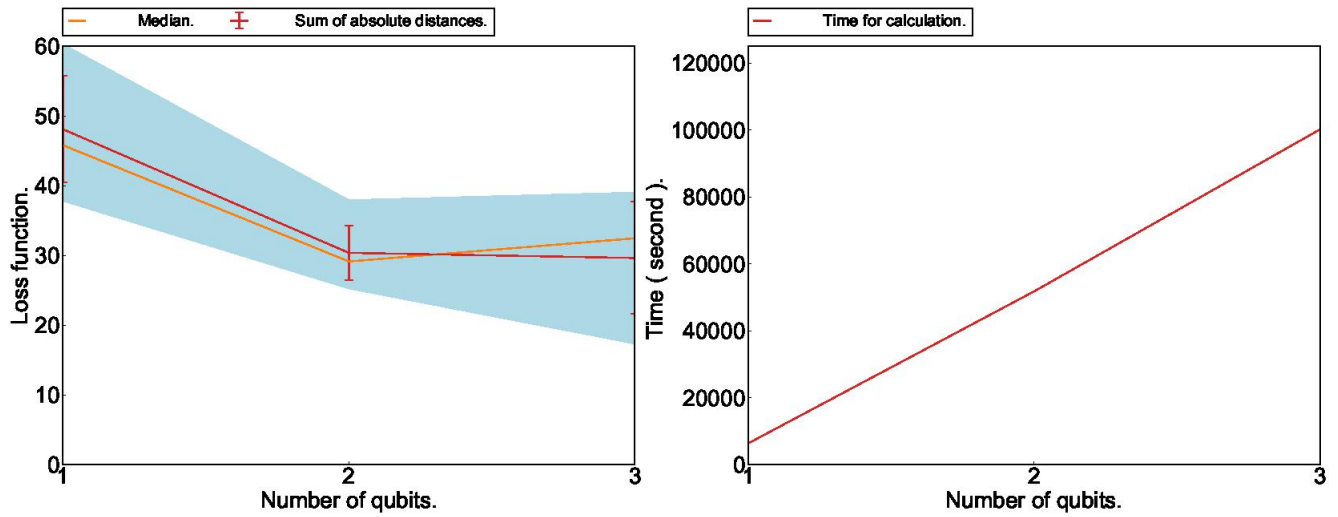


Figure 10. (Left) Number of layers vs. sum of absolute distances using EVQKAN on classification problem with $N_q = 3$ and COBYLA. (Right) Number of layers vs. elapsed time.

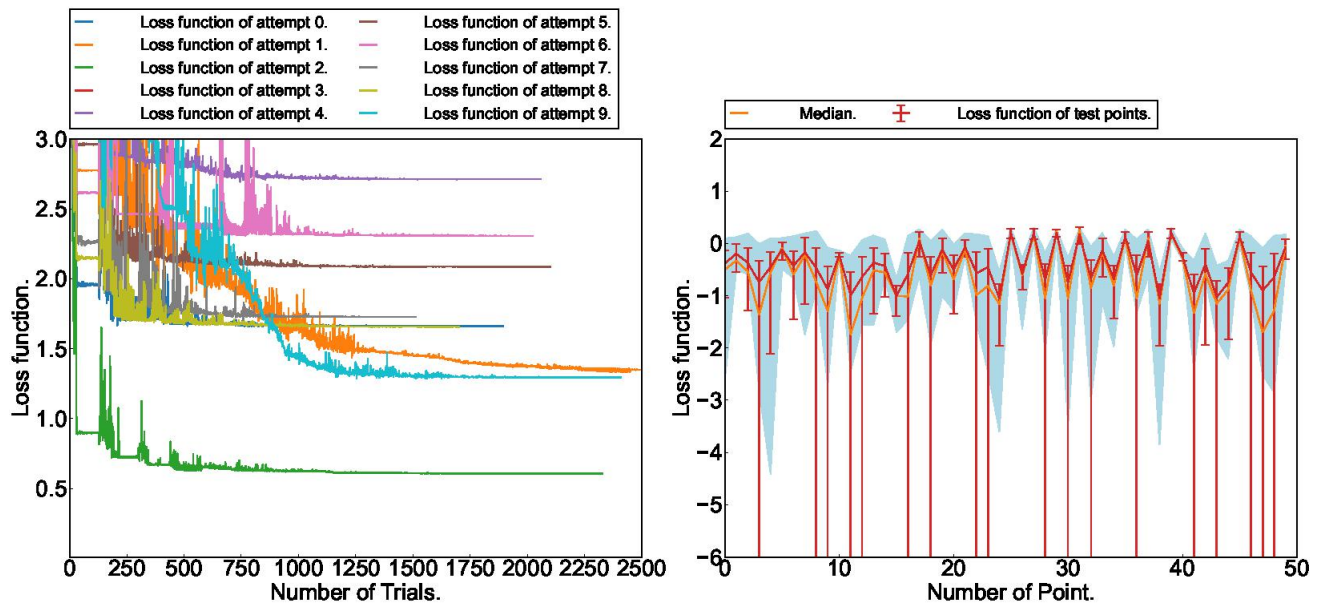


Figure 11. (Left) Number of trials vs. loss functions for optimization attempts on classification problem by EVQKAN in case the ansatz is transposed and the number of layers is 1. (Right) Number of test points vs. average and median of loss functions (absolute distances) in log10 scale of test points on EVQKAN optimization.

5 Concluding Remarks

In this paper, we demonstrated the EVQKAN for fitting elementary equations and classifying points, and it is revealed that it has the potential to deal with machine learning problems the same as or more than QNN and VQKAN. Our key findings are significant accuracy of EVQKAN for learned data even EVQKAN is more trapped by overfitting, and further accuracy than conventional QNN. However, the calculation time increases exponentially by increasing the number of layers exchanged for the prominent accuracy improvement. The next objective is to simplify the circuit, including reducing the number of qubits by block encoding and quantization. Benchmarking of accuracy and resilience against noise with VQKAN and Adaptive VQKAN is also important.

References

1. Yu, Y., Si, X., Hu, C. & Zhang, J. A Review of Recurrent Neural Networks: LSTM Cells and Network Architectures. *Neural Comput.* **31**, 1235–1270, DOI: [10.1162/neco_a_01199](https://doi.org/10.1162/neco_a_01199) (2019). https://direct.mit.edu/neco/article-pdf/31/7/1235/1053200/neco_a_01199.pdf.
2. Masood, A., Naseem, U., Rashid, J., Kim, J. & Razzak, I. Review on enhancing clinical decision support system using machine learning. *CAAI Transactions on Intell. Technol.* **n/a**, DOI: <https://doi.org/10.1049/cit2.12286> (2024). <https://ietresearch.onlinelibrary.wiley.com/doi/pdf/10.1049/cit2.12286>.
3. Xing, Y. & Zhu, J. Deep learning-based action recognition with 3d skeleton: A survey. *CAAI Transactions on Intell. Technol.* **6**, 80–92, DOI: <https://doi.org/10.1049/cit2.12014> (2021). <https://ietresearch.onlinelibrary.wiley.com/doi/pdf/10.1049/cit2.12014>.
4. Ghosh, A., Chakraborty, D. & Law, A. Artificial intelligence in internet of things. *CAAI Transactions on Intell. Technol.* **3**, 208–218, DOI: <https://doi.org/10.1049/trit.2018.1008> (2018). <https://ietresearch.onlinelibrary.wiley.com/doi/pdf/10.1049/trit.2018.1008>.
5. Liu, Z. *et al.* KAN: Kolmogorov-Arnold Networks. *arXiv e-prints* arXiv:2404.19756, DOI: [10.48550/arXiv.2404.19756](https://doi.org/10.48550/arXiv.2404.19756) (2024). [2404.19756](https://arxiv.org/abs/2404.19756).
6. Cang, Y., liu, Y. h. & Shi, L. Can KAN Work? Exploring the Potential of Kolmogorov-Arnold Networks in Computer Vision. *arXiv e-prints* arXiv:2411.06727, DOI: [10.48550/arXiv.2411.06727](https://doi.org/10.48550/arXiv.2411.06727) (2024). [2411.06727](https://arxiv.org/abs/2411.06727).
7. Han, D., Li, Y. & Denzler, J. KAN See Your Face. *arXiv e-prints* arXiv:2411.18165, DOI: [10.48550/arXiv.2411.18165](https://doi.org/10.48550/arXiv.2411.18165) (2024). [2411.18165](https://arxiv.org/abs/2411.18165).
8. Kim, T., Girard, A. & Kolmanovsky, I. CIKAN: Constraint Informed Kolmogorov-Arnold Networks for Autonomous Spacecraft Rendezvous using Time Shift Governor. *arXiv e-prints* arXiv:2412.03710, DOI: [10.48550/arXiv.2412.03710](https://doi.org/10.48550/arXiv.2412.03710) (2024). [2412.03710](https://arxiv.org/abs/2412.03710).
9. Bandyopadhyay, Y., Avlani, H. & Zhuang, H. L. Kolmogorov-Arnold Neural Networks for High-Entropy Alloys Design. *arXiv e-prints* arXiv:2410.08452, DOI: [10.48550/arXiv.2410.08452](https://doi.org/10.48550/arXiv.2410.08452) (2024). [2410.08452](https://arxiv.org/abs/2410.08452).
10. Kou, W. & Chen, X. Machine Learning Insights into Quark-Antiquark Interactions: Probing Field Distributions and String Tension in QCD. *arXiv e-prints* arXiv:2411.14902, DOI: [10.48550/arXiv.2411.14902](https://doi.org/10.48550/arXiv.2411.14902) (2024). [2411.14902](https://arxiv.org/abs/2411.14902).
11. Jahin, M. A., Akmol Masud, M., Mridha, M. F., Aung, Z. & Dey, N. KACQ-DCNN: Uncertainty-Aware Interpretable Kolmogorov-Arnold Classical-Quantum Dual-Channel Neural Network for Heart Disease Detection. *arXiv e-prints* arXiv:2410.07446, DOI: [10.48550/arXiv.2410.07446](https://doi.org/10.48550/arXiv.2410.07446) (2024). [2410.07446](https://arxiv.org/abs/2410.07446).
12. Tang, T., Chen, Y. & Shu, H. 3D U-KAN Implementation for Multi-modal MRI Brain Tumor Segmentation. *arXiv e-prints* arXiv:2408.00273, DOI: [10.48550/arXiv.2408.00273](https://doi.org/10.48550/arXiv.2408.00273) (2024). [2408.00273](https://arxiv.org/abs/2408.00273).
13. Wakaura, H., Bayu Suksmono, A. & Mulyawan, R. Variational quantum kolmogorov-arnold network. *Res. Sq.* DOI: [10.21203/rs.3.rs-4504342/v3](https://doi.org/10.21203/rs.3.rs-4504342/v3) (2024). PREPRINT (Version 3).
14. Ivashkov, P., Huang, P.-W., Koor, K., Pira, L. & Rebentrost, P. QKAN: Quantum Kolmogorov-Arnold Networks. *arXiv e-prints* arXiv:2410.04435, DOI: [10.48550/arXiv.2410.04435](https://doi.org/10.48550/arXiv.2410.04435) (2024). [2410.04435](https://arxiv.org/abs/2410.04435).
15. Motlagh, D. & Wiebe, N. Generalized Quantum Signal Processing. *PRX Quantum* **5**, 020368, DOI: [10.1103/PRXQuantum.5.020368](https://doi.org/10.1103/PRXQuantum.5.020368) (2024). [2308.01501](https://arxiv.org/abs/2308.01501).
16. Kundu, A., Sarkar, A. & Sadhu, A. KANQAS: Kolmogorov-Arnold Network for Quantum Architecture Search. *EPJ Quantum Technol.* **11**, 76, DOI: [10.1140/epjqt/s40507-024-00289-z](https://doi.org/10.1140/epjqt/s40507-024-00289-z) (2024). [2406.17630](https://arxiv.org/abs/2406.17630).

17. Kassal, I., Whitfield, J. D., Perdomo-Ortiz, A., Yung, M.-H. & Aspuru-Guzik, A. Simulating chemistry using quantum computers. *Annu. Rev. Phys. Chem.* **62**, 185–207, DOI: [10.1146/annurev-physchem-032210-103512](https://doi.org/10.1146/annurev-physchem-032210-103512) (2011). <https://doi.org/10.1146/annurev-physchem-032210-103512>.
18. McClean, J. R., Romero, J., Babbush, R. & Aspuru-Guzik, A. The theory of variational hybrid quantum-classical algorithms. *New J. Phys.* **18**, 023023, DOI: [10.1088/1367-2630/18/2/023023](https://doi.org/10.1088/1367-2630/18/2/023023) (2016).
19. Grimsley, H. R., Economou, S. E., Barnes, E. & Mayhall, N. J. An adaptive variational algorithm for exact molecular simulations on a quantum computer. *Nat. Commun.* **10**, 3007, DOI: [10.1038/s41467-019-10988-2](https://doi.org/10.1038/s41467-019-10988-2) (2019). [1812.11173](https://arxiv.org/abs/1812.11173).
20. Parrish, R. M., Hohenstein, E. G., McMahan, P. L. & Martinez, T. J. Hybrid Quantum/Classical Derivative Theory: Analytical Gradients and Excited-State Dynamics for the Multistate Contracted Variational Quantum Eigensolver. *arXiv e-prints* arXiv:1906.08728 (2019). [1906.08728](https://arxiv.org/abs/1906.08728).
21. Rebentrost, P., Mohseni, M. & Lloyd, S. Quantum Support Vector Machine for Big Data Classification. *Phys. Rev. Lett.* **113**, 130503, DOI: [10.1103/PhysRevLett.113.130503](https://doi.org/10.1103/PhysRevLett.113.130503) (2014). [1307.0471](https://arxiv.org/abs/1307.0471).
22. Khoshaman, A. *et al.* Quantum variational autoencoder. *Quantum Sci. Technol.* **4**, 014001, DOI: [10.1088/2058-9565/aada1f](https://doi.org/10.1088/2058-9565/aada1f) (2019). [1802.05779](https://arxiv.org/abs/1802.05779).
23. Havlíček, V. *et al.* Supervised learning with quantum-enhanced feature spaces. *Nature* **567**, 209–212, DOI: [10.1038/s41586-019-0980-2](https://doi.org/10.1038/s41586-019-0980-2) (2019). [1804.11326](https://arxiv.org/abs/1804.11326).
24. Abel, S., Criado, J. C. & Spannowsky, M. Completely quantum neural networks. *Phys. Rev. A* **106**, 022601, DOI: [10.1103/PhysRevA.106.022601](https://doi.org/10.1103/PhysRevA.106.022601) (2022). [2202.11727](https://arxiv.org/abs/2202.11727).
25. Kwak, Y. *et al.* Quantum Distributed Deep Learning Architectures: Models, Discussions, and Applications. *arXiv e-prints* arXiv:2202.11200 (2022). [2202.11200](https://arxiv.org/abs/2202.11200).
26. Benedetti, M., Coyle, B., Fiorentini, M., Lubasch, M. & Rosenkranz, M. Variational Inference with a Quantum Computer. *Phys. Rev. Appl.* **16**, 044057, DOI: [10.1103/PhysRevApplied.16.044057](https://doi.org/10.1103/PhysRevApplied.16.044057) (2021). [2103.06720](https://arxiv.org/abs/2103.06720).
27. Wang, Z. T., Ashida, Y. & Ueda, M. Deep Reinforcement Learning Control of Quantum Cartpoles. *Phys. Rev. Lett.* **125**, 100401, DOI: [10.1103/PhysRevLett.125.100401](https://doi.org/10.1103/PhysRevLett.125.100401) (2020). [1910.09200](https://arxiv.org/abs/1910.09200).
28. Yang, D., Xiao, Z. & Yu, W. Boosting the Adversarial Transferability of Surrogate Model with Dark Knowledge. *arXiv e-prints* arXiv:2206.08316 (2022). [2206.08316](https://arxiv.org/abs/2206.08316).
29. Mitarai, K., Negoro, M., Kitagawa, M. & Fujii, K. Quantum circuit learning. *Phys. Rev. A* **98**, 032309, DOI: [10.1103/PhysRevA.98.032309](https://doi.org/10.1103/PhysRevA.98.032309) (2018).
30. McClean, J. R., Boixo, S., Smelyanskiy, V. N., Babbush, R. & Neven, H. Barren plateaus in quantum neural network training landscapes. *Nat. Commun.* **9**, 4812, DOI: [10.1038/s41467-018-07090-4](https://doi.org/10.1038/s41467-018-07090-4) (2018).
31. Nakanishi, K. M., Mitarai, K. & Fujii, K. Subspace-search variational quantum eigensolver for excited states. *arXiv e-prints* arXiv:1810.09434 (2018). [1810.09434](https://arxiv.org/abs/1810.09434).
32. Kosugi, T. & Matsushita, Y.-i. Linear-response functions of molecules on a quantum computer: Charge and spin responses and optical absorption. *Phys. Rev. Res.* **2**, 033043, DOI: [10.1103/PhysRevResearch.2.033043](https://doi.org/10.1103/PhysRevResearch.2.033043) (2020).
33. Kato, T. <https://github.com/Qaqarot>. Opensource software development kit (2018).
34. Wakaura, H., Mulyawan, R. & Suksmono, A. B. Adaptive Variational Quantum Kolmogorov-Arnold Network. *arXiv e-prints* arXiv:2503.21336 (2025). [2503.21336](https://arxiv.org/abs/2503.21336).
35. Sengupta, R., Adhikary, S., Oseledets, I. & Biamonte, J. Tensor networks in machine learning. *arXiv e-prints* arXiv:2207.02851, DOI: [10.48550/arXiv.2207.02851](https://doi.org/10.48550/arXiv.2207.02851) (2022). [2207.02851](https://arxiv.org/abs/2207.02851).
36. Moussa, C., Patel, Y. J., Dunjko, V., Bäck, T. & van Rijn, J. N. Hyperparameter importance and optimization of quantum neural networks across small datasets. *Mach. Learn.* **113**, 1941–1966, DOI: [10.1007/s10994-023-06389-8](https://doi.org/10.1007/s10994-023-06389-8) (2024).
37. Hirai, H. Practical application of quantum neural network to materials informatics. *Sci. Reports* **14**, 8583, DOI: [10.1038/s41598-024-59276-0](https://doi.org/10.1038/s41598-024-59276-0) (2024).